T2-Weighted MR Characteristics of Internal Auditory Canal Masses

Melanie B. Fukui, Jane L. Weissman, Hugh D. Curtin, and Emanuel Kanal

PURPOSE: To determine whether masses of the internal auditory canal are hypointense relative to cerebrospinal fluid, and therefore visible, on fast spin-echo T2-weighted MR images. **METHODS:** Forty-six patients had 50 masses of the internal auditory canal, identified initially on contrast-enhanced MR images, that were evaluated retrospectively for signal intensity of the mass with respect to cerebrospinal fluid and for visibility of the neural elements within the internal auditory canal on T2-weighted images. **RESULTS:** Forty-seven of 50 masses were clearly identified on T2-weighted images. Three small abnormalities (2 to 4 mm) were not seen with confidence on T2-weighted images. However, on close inspection of these three masses, the small abnormality on contrast-enhanced MR images corresponded to a hypointense focus on T2-weighted images. All 50 masses were hypointense relative to cerebrospinal fluid on T2-weighted images. **CONCLUSION:** All masses of the internal auditory canal in this study were hypointense relative to cerebrospinal fluid on T2-weighted images, and were therefore visible.

Index terms: Neuroma; Temporal bone, magnetic resonance

AJNR Am J Neuroradiol 17:1211–1218, August 1996

Contrast-enhanced magnetic resonance (MR) imaging is currently considered the standard of reference for the diagnosis of masses of the internal auditory canal (IAC) (1–5). If T2-weighted MR imaging proves to be a sensitive method for detecting masses (presumed acoustic schwannomas) of the IAC, then contrast-enhanced MR imaging may be reserved for cases in which the nerves are not completely displayed, creating ambiguity on T2-weighted images. Initial screening with T2-weighted imaging combined with unenhanced relatively T1-weighted imaging could result in a significant time savings.

Exploiting the cerebrospinal fluid (CSF)–tumor interface is crucial in the detection of small masses of the IAC (6) on T2-weighted images. If T2-weighted imaging is to be an effective (that is, sensitive) screening study, the following criteria must be met: first, all masses must be hypointense relative to CSF on T2-weighted images in order to be conspicuous (6) and, second, if a mass is not clearly seen on the T2-weighted images, there must be some abnormality on the T2-weighted study, such as thickening of the nerves or indefinite visibility of the nerves, that prompts the use of contrast material. The purpose of this study was to determine whether IAC masses are hypointense relative to CSF, and therefore visible, on high-resolution fast spin-echo T2-weighted images.

Materials and Methods

Patient Cohort

A review of the clinical records from July 1988 to May 1995 revealed 46 patients (22 women and 24 men) with 50 masses of the IAC that showed enhancement on T1-weighted images after administration of contrast material. These cases were included in the study. All patients had also undergone T2-weighted imaging. Twenty-three of the 50 masses were purely intracanalicular lesions.

The abnormalities, originally detected on contrast-enhanced MR imaging, ranged in size from 2 × 2 mm to 38 × 40 mm (measured on T2-weighted images). Clinical

Received October 11, 1995; accepted after revision February 16, 1996.

Presented in part at the annual scientific conference of the American Society of Head and Neck Radiology, Pittsburgh, Pa, May 1995.

From the Departments of Radiology (M.B.F., J.L.W., E.K.) and Otolaryngology (J.L.W.), University of Pittsburgh (Pa) Medical Center; and the Department of Radiology, Massachusetts Eye and Ear Infirmary, Boston (H.D.C.).

Address reprint requests to M. B. Fukui, MD, Department of Radiology, University of Pittsburgh Medical Center, 200 Lothrop St, Pittsburgh, PA 15213.

AJNR 17:1211–1218, Aug 1996 0195-6108/96/1707–1211

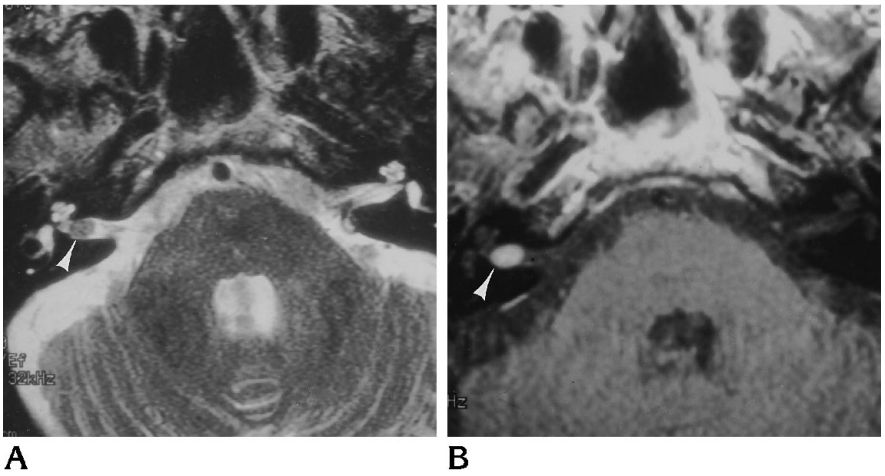

Fig 1. Typical intracanalicular mass of the IAC.

Axial fast spin-echo T2-weighted (4000/108 effective) MR image (*A*) shows a small (3 × 6 mm) hypointense mass (*arrowhead*) in the right IAC, which corresponds to the enhancing abnormality (*arrowhead*) on the axial contrast-enhanced T1-weighted (633/23) image (*B*). Note that in the normal left IAC the neural elements are clearly identified and are surrounded by bright CSF on the T2-weighted image.

information was available in 43 of the patients. Seventeen of these 43 had sensorineural hearing loss and 14 had hearing loss, type not specified. Presenting disorders in the remaining 12 patients included neuropathy of the fifth cranial nerve, balance difficulty, tinnitus, vertigo, or signs and symptoms of increased intracranial pressure.

Pathologic samples were available for 21 of the 50 lesions: 20 were vestibular schwannomas and one was a meningioma. There were 29 lesions for which there was no histologic diagnosis: 24 of these had follow-up imaging, which showed a persistent or enlarging abnormality over at least 6 months. There were five masses that ranged in size from 7 to 33 mm in maximum diameter for which neither pathologic samples nor sequential images were available.

Scan Technique

All but nine patients underwent high-resolution fast spin-echo T2-weighted MR imaging on a 1.5-T unit equipped with a head coil. Imaging parameters were as follows: 3000–4300/80–114/4 (repetition time [TR]/echo time [TE]/excitations), echo train length of 8 to 16; field of view of 18 × 18 cm; matrix of 512 × 256; 3-mm section thickness with a 0.5-mm intersection gap; and an acquisition time of approximately 4 minutes. The other nine patients had T2-weighted studies that were determined to be of sufficient quality for inclusion in the study by virtue of the neural elements being visible in the IAC. These T2-weighted studies were obtained with the following (variable) parameters: 2316–2875/80–102/2; field of view of 18 to 20 cm; matrix of 256 × 192; and a 3-mm to 5-mm section thickness with a 0-mm to 1-mm intersection gap. All patients also had T1-weighted studies after intravenous administration of 0.1 mmol/kg of contrast material. Parameters for the T1-weighted studies were 400–783/12–30/1–2; field of view of 18 to 20; matrix of 256 × 192–256; section thickness of 3 mm, interleaved (with a 1.0-mm intersection gap) to 5 mm with 1-mm intersection gap. Axial images were obtained in all cases; coronal images were added in some cases at the discretion of the radiologist who reviewed the initial images at the monitor. Twenty-four of the 50 T2-weighted studies were obtained after administration of contrast material. The T2-weighted studies of the remaining 26 lesions were obtained before administration of contrast material. In two cases, T2-weighted studies were performed before and after contrast administration to determine whether there was a detectable change in the lesion's signal intensity due to contrast material that would affect interpretation of the results. In addition, the difference in T2 signal characteristics of vestibular schwannomas before and after administration of contrast material was calculated using a computer program.

The T2-weighted images were evaluated for signal intensity of the IAC mass with respect to CSF (lesion conspicuity) and for visibility of the neural elements in the IAC (nerve visibility). The reviewers were not blinded to the findings on the contrast-enhanced MR images. Heterogeneous lesions were characterized according to their lowest signal intensity component. Signal intensity of lesions on T2-weighted images was rated according to the following scale: 1 = hypointense relative to gray matter; 2 = hypointense relative to CSF; 3 = isointense with CSF; 4 = hyperintense relative to CSF. Three unusual cases in which the lesion was not considered to be equally obvious on both contrast-enhanced and T2-weighted images by the initial reader were subsequently reviewed by two other radiologists who specialize in head and neck imaging.

Results

Lesion Conspicuity

Forty-seven of 50 lesions were clearly identified as masses on T2-weighted images. All 47 were either entirely or partly hypointense relative to CSF on T2-weighted images. Forty-two lesions were scored as 1 (hypointense relative to gray matter); eight lesions were scored as 2 (hypointense relative to CSF but hyperintense

Fig 2. The first of three equivocal cases on T2-weighted images.

Axial fast spin-echo T2-weighted (4000/108 effective) MR images (*A* and *B*) show that both IACs are small so that there is scant CSF in the IACs. The paucity of contrasting signal from CSF makes it difficult to determine whether the neural elements are normal. There is a tiny hypointense focus in the right IAC (*small arrowheads*), which corresponds to the small enhancing abnormality (*large arrowhead*) on the axial T1-weighted (400/15) contrast-enhanced image (*C*).

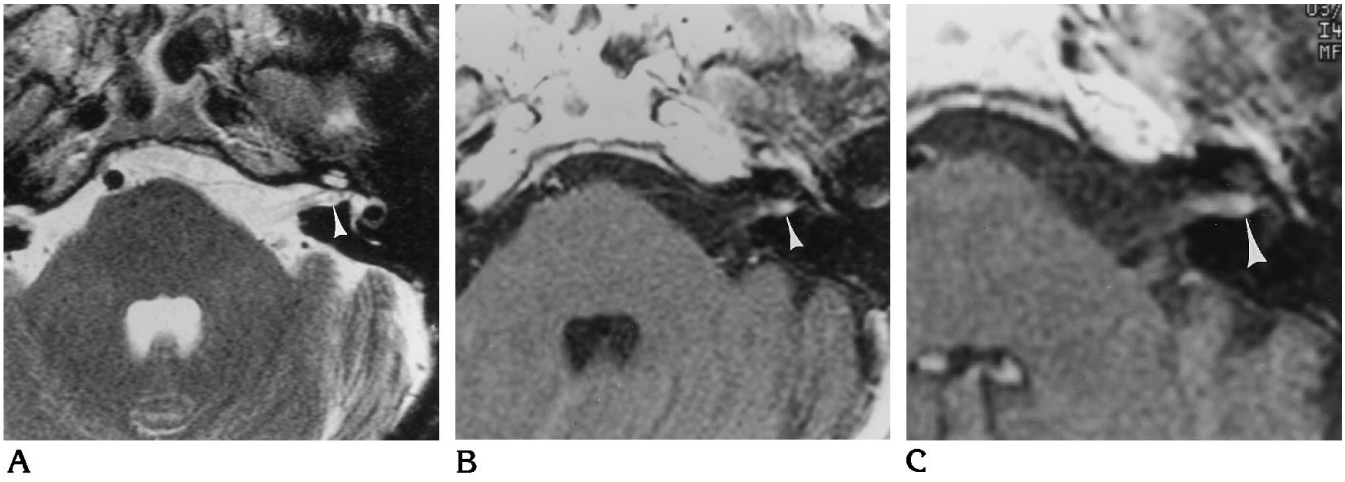

Fig 3. The second case in which the lesion was not obvious on T2-weighted images.

Axial fast spin-echo T2-weighted (4000/108 effective) MR image (*A*) shows a hypointense nodule of the left inferior vestibular nerve near the fundus of the IAC (*arrowhead*), which corresponds to the enhancement (*arrowhead*) on the axial contrast-enhanced T1-weighted (400/12) image (*B*). The enhancement in the left IAC did not represent neuritis, since it was present on the axial contrast-enhanced T1-weighted (433/15) image obtained 1 year earlier (*arrowhead* in *C*).

with respect to gray matter). No lesion received a score of 3 or 4. A typical example of an intracanalicular lesion (3 × 6 mm) is shown in Figure 1.

The masses ranged in maximum diameter (as measured on T2-weighted images) from 3 to 40 mm. Eleven of the 47 lesions were between 6 and 10 mm in maximum diameter; the remaining 31 of 47 were greater than 10 mm.

Eight of 50 lesions were 5 mm or less. Five of these were identified with confidence on T2-weighted images and ranged in maximum diameter from 3 to 4 mm. The remaining three small (2 × 2 mm; 3 × 3 mm; 3 × 4 mm) lesions were considered to be equivocal cases, since the initial reviewer deemed that these lesions were sufficiently small to risk being missed on T2-weighted images if contrast-enhanced MR images were not available for correlation. In these three cases a tiny (2 to 4 mm) enhancing abnormality on the contrast-enhanced study was seen retrospectively by all three reviewers to correspond to a hypointense focus on the T2-weighted study. In these cases the lesion on

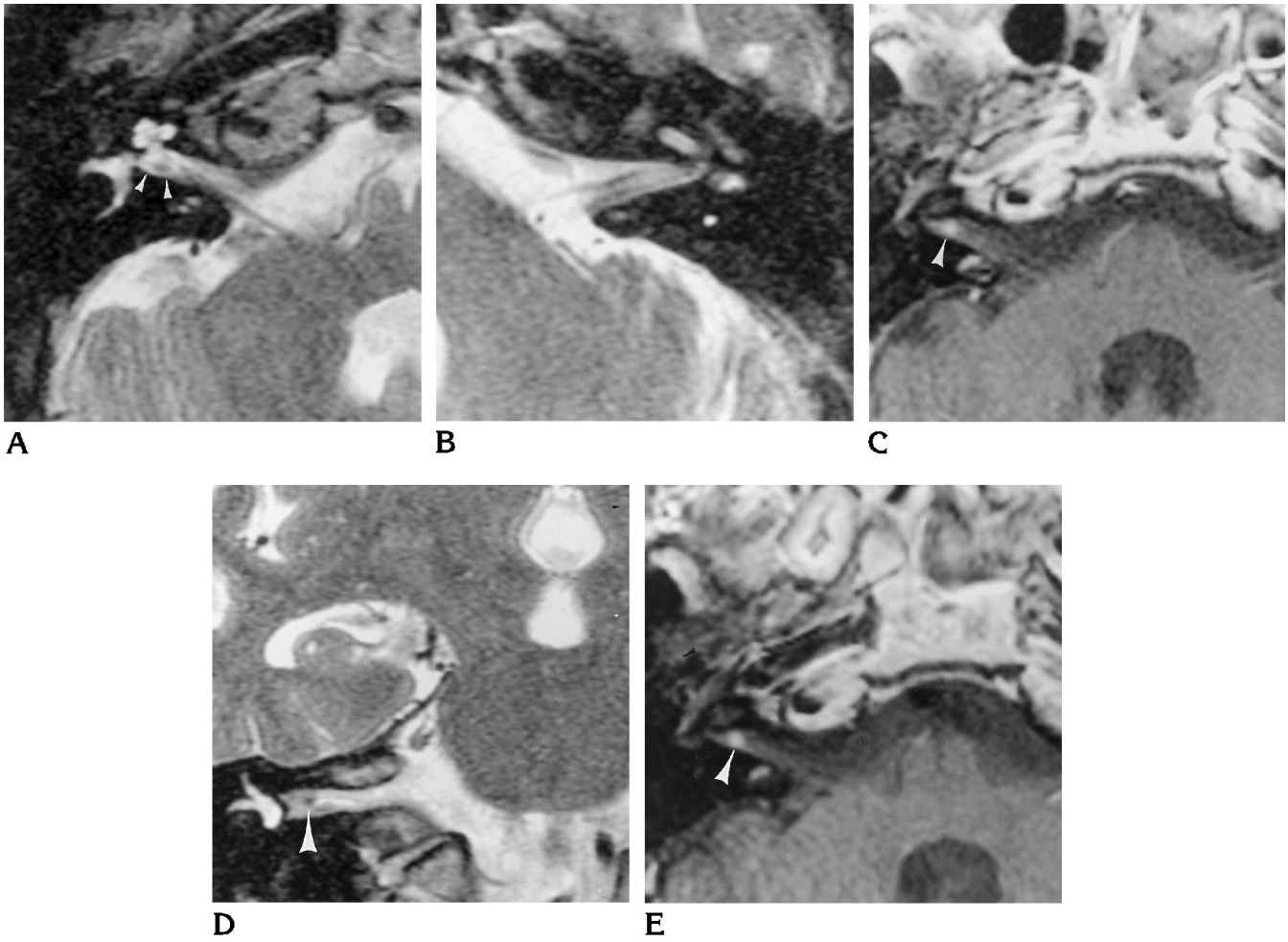

Fig 4. The last of the three equivocal cases on T2-weighted images.

Axial fast spin-echo T2-weighted (4000/108 effective) MR images of right (*A*) and left (*B*) IAC show the cochlear nerve well, but the right inferior vestibular nerve is not seen in its entirety within the IAC. There is a hypointense focus in the right IAC (*small arrowheads*), which corresponds to the enhancement (*arrowhead*) on the axial contrast-enhanced T1-weighted (400/12) image (*C*). In *B*, the normal left cochlear and inferior vestibular nerves are seen throughout their course in the IAC, surrounded by CSF.

D, Coronal fast spin-echo T2-weighted (4000/108 effective) image confirms the hypointense lesion in the right IAC (*arrowhead*).

E, Axial T1-weighted (600/23) image (initial study) shows enhancement in the right IAC (*arrowhead*), which persisted for 1 year.

the contrast-enhanced study was 2 to 4 mm and was located in the fundus of the IAC (Figs 2–4).

In two cases, fast spin-echo T2-weighted imaging was performed before and after administration of contrast material to determine whether the contrast material shortened the T2 signal of the lesion sufficiently to cause a detectable decrease in the lesion's signal intensity on T2-weighted images. The small difference in signal intensity predicted by the computer program for T2-weighted images before versus after contrast administration matched our impression of the two cases in which T2-weighted imaging was performed before and after contrast administration. In these two cases no difference in the lesion's signal intensity could be detected between the precontrast and postcontrast T2-weighted studies (Fig 5).

Nerve Visibility

In 48 of the 50 IACs that were abnormal on contrast-enhanced MR images, the nerves were not identified within the IAC on the T2-weighted images. In the remaining two cases, the neural elements were either thickened or were not seen in their entirety in the IAC on T2-weighted images (Figs 3 and 4). In one of these two cases (Fig 3), there was a tiny nodule along the course of the left inferior vestibular nerve that corresponded to the enhancing abnormality on the contrast-enhanced images. In the second case

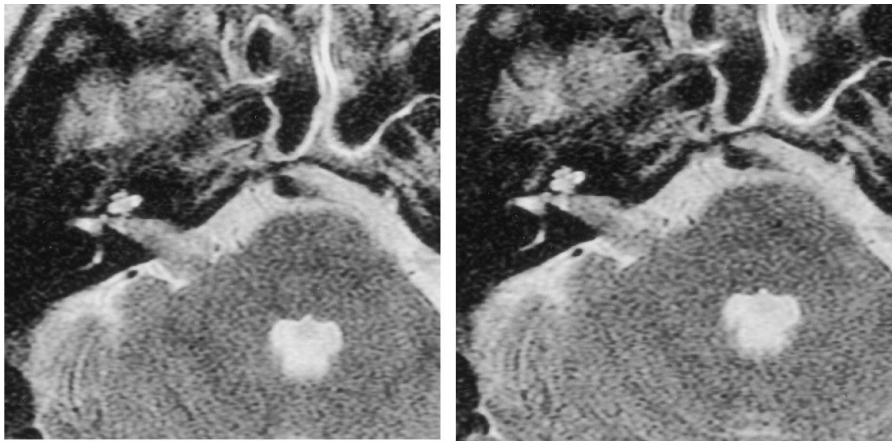

Fig 5. Axial fast spin-echo T2-weighted (4000/108 effective) MR images of right IAC show mass before (*A*) and after (*B*) administration of contrast material.

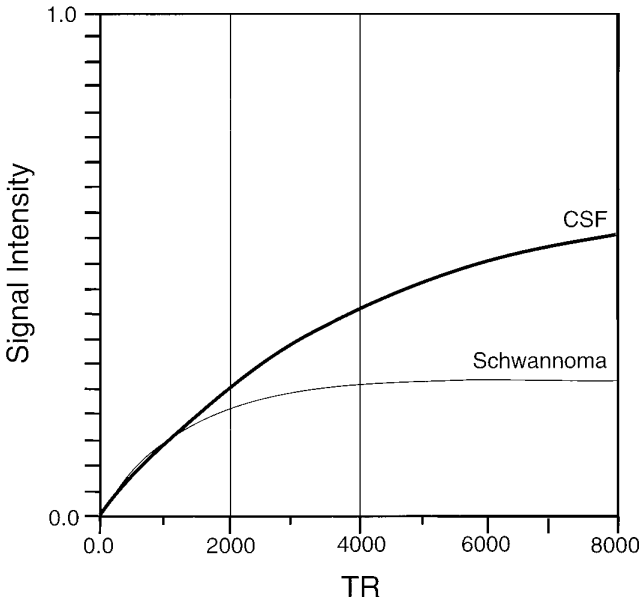

Fig 6. Relative signal intensities of vestibular schwannoma and CSF at TRs of 2000 and 4000, with TE constant at 108.

(Fig 4), there was a hypointense focus in the expected location of Scarpa's ganglion that corresponded to the abnormal enhancement on the contrast-enhanced image, and the right inferior vestibular nerve was not seen throughout its entire course in the IAC. There was no pathologic correlation for these three small lesions, which are being managed with follow-up imaging.

In all 42 patients with unilateral masses, the uninvolved IAC was used as a control. In these cases the nerves were seen and were normal on T2-weighted images in all but one case. In this one case, the nerves could not be identified clearly throughout their course on T2-weighted images, because the IACs were very small bilaterally, and the surrounding CSF was insufficient to provide contrast with the nerves (Fig 2A and B).

Discussion

All IAC masses in this series had a component that was hypointense relative to CSF on T2-weighted images. In all cases a focus of decreased signal intensity relative to CSF correlated with the abnormal enhancement on contrast-enhanced MR images. T2-weighted images clearly showed 47 of 50 lesions previously detected by contrast-enhanced MR imaging. Although this study is limited in that it lacks complete pathologic correlation, the lesions described were managed clinically as if they were acoustic (vestibular) schwannomas, in most cases on the basis of follow-up imaging when histologic diagnosis was not possible. All of the small (< 5 mm) lesions in this study had follow-up imaging, which showed a persistent or enlarging mass, and so were considered likely to be schwannomas. In five cases there was neither follow-up imaging nor pathologic correlation available; however, the lesion size (7 to 33 mm) supported a diagnosis of neoplasm rather than neuritis.

Vestibular schwannomas are often described as isointense or hyperintense masses on T2-weighted images (4, 6–8) and therefore are notoriously difficult to detect on T2-weighted images. The disparity in the literature regarding the conspicuity of IAC masses on T2-weighted images most likely arises from the broad range of imaging parameters used: 2000/20–90 (4);

2000/80 (6, 7); and 2200/70 (8). A few authors, however, have reported a high rate of detection of IAC masses on T2-weighted images (9, 10). Those who reported that IAC masses are reliably detected on T2-weighted images used parameters of 3000/100 (effective) (9) or 4000/84 (effective) (10) with fast spin-echo and 4000/120–140 with conventional spin-echo imaging (E. Kanal, "High Resolution 1.5 Tesla MRI of Acoustic Neuromas and Cerebello-pontine Angle Tumors," presented at the Fifth Annual Meeting of the Society of Magnetic Resonance Imaging in Medicine, Montreal, Canada, August 1986). The long TR/TE used in this study emphasizes differences in T2 values between CSF and IAC masses (Fig 6). The long T2 value of CSF is exploited in sequences using a long TR (>3000) and long TE (>100), since the CSF remains bright while most other tissues have lost signal at TEs of greater than 100 and are hypointense with respect to CSF. At TR values of 2000 to 2500, T1 contrast plays an important role. CSF has a very long T1 value at 1.5 T, which results in relatively lower signal intensity of CSF at TRs of 2000 to 2500 compared with longer TRs of 4000 or greater.

The low signal of schwannomas may be related to a preponderance of Antoni type A tissue, which is denser than Antoni type B tissue on histologic sections. High cellularity of small vestibular schwannomas has been described (11) and may provide the explanation for the homogeneously low signal intensity of the IAC lesions that were smaller than 5 mm in this series. High cellularity resulting in hypointensity on T2-weighted images has also been described in central nervous system lymphoma (12) and malignant parotid tumors (13).

Several of the small lesions in this series occurred in the fundus of the IAC, raising the question of the site of origin of vestibular schwannomas. The traditional thinking is that vestibular schwannomas arise from the glial–Schwann cell junction in the IAC (14–17). The glial–Schwann cell transition (Obersteiner-Redlich zone) often occurs near the vestibular (Scarpa's) ganglion (18), but can vary in its location within the IAC (16–22). Vestibular schwannomas can also originate in the sensory ganglion and distal nerve end (23). The sensory ganglion of the vestibular nerve (Scarpa's ganglion), which is near the fundus of the IAC along the course of the inferior vestibular nerve, is a more common site of origin of vestibular schwannomas than is the glial–Schwann cell junction (18, 24, 25). Although, in general, the concentration of Schwann cells has not been correlated with the distribution of vestibular schwannomas, there is a preponderance of Schwann cells at the vestibular ganglion (20). These data correspond to the distribution of small intracanalicular tumors reported previously (26) and with the location of small lesions at the fundus of the IAC in this series.

Some authors have objected to the use of T2-weighted images in evaluating vestibular schwannomas because of CSF flow effects in the cerebellopontine angle cistern and IAC (1, 27), high-protein CSF simulating tumor (3), and an inability to distinguish between the tumor and adjacent CSF (6, 27). Although many (n = 37) of the tumors in this series were heterogeneous in signal intensity on T2-weighted images, all of the lesions had a component that was hypointense relative to CSF on T2-weighted images. In some of the cases with large heterogeneous lesions it was difficult to delineate the exact border of the lesion on the basis of T2-weighted images alone. When the unenhanced T1-weighted studies were available, however, the border was readily apparent, since the mass was hyperintense with respect to CSF on T1-weighted images. In addition, in no case of a heterogeneous mass was there a problem of lesion detection; the mass was obvious in those cases, and therefore contrast-enhanced T1-weighted images would have been indicated for definitive evaluation of the extent of the lesion. CSF flow in the cerebellopontine angle cistern did not have an impact on lesion detection in this series, although flow effects did reduce the contrast at the interface between the CSF in the cerebellopontine angle cistern and the cerebellopontine angle component of the lesion. In those cases, however, the mass was sufficiently large that it was not a matter of detection but of demarcation of the lesion's borders, which could again be accomplished by using T1-weighted images either with or without contrast material. In the cases in which the signal intensity of the margin of the cerebellopontine angle component was not clearly differentiated from CSF, the IAC component was readily identified as hypointense relative to CSF on T2-weighted images. The main artifact that created limitations in this series (since the section thickness on the T2-weighted images was 3

mm) was partial volume averaging, which has been cited by others (9). Thinner-section T2-weighted images might obviate this shortcoming in the future.

Potential sources of error in this study are that it was retrospective, that there was a single initial reviewer of the MR images, and that the uninvolved IAC served as the control for each examination. The larger purpose of our study was to contribute to understanding the appearance of IAC lesions on T2-weighted MR images; the more specific objective was to establish the relative signal characteristics of IAC masses with respect to CSF, and therefore their visibility, on T2-weighted images. A simple correlation study was performed to that end. The study design introduced bias, since the initial evaluation included the T2-weighted images and the contrast-enhanced MR images. The initial reviewer classified cases as definite IAC lesions on T2-weighted images if the mass was as obvious on T2-weighted images as it was on the contrast-enhanced MR images. Cases were considered to be equivocal if the lesion was more difficult to see on T2-weighted images than on contrast-enhanced images. Equivocal cases were then reviewed by two additional radiologists specializing in head and neck imaging. Since only those cases with high signal on postcontrast T1-weighted images were evaluated in this series, some types of disease, such as epidermoid, were excluded. None of the lesions in this series had signal characteristics of methemoglobin or fat. Epidermoid, methemoglobin, and fat could all have a long T2 and appear bright on T2-weighted images. Using unenhanced T1-weighted images would exclude rare diagnoses, such as lipoma of the IAC, in equivocal cases that lacked pathologic confirmation of vestibular schwannoma (28). Prospective evaluation of T2-weighted images in a double-blind fashion with a larger patient cohort and a large control population could address these limitations.

Three small lesions (2 to 4 mm) were difficult to evaluate on T2-weighted images alone and were more obvious on contrast-enhanced images. The difficulty in evaluating small lesions was related to size and not to signal intensity. The scanning techniques used in this series varied somewhat, since cases were accumulated over several years in this retrospective study. The section thickness (3 mm with a 0.5-mm intersection gap) caused limitations in imaging small lesions and some partial volume effects. Coronal T2-weighted imaging was helpful in one of the equivocal cases (Fig 4D). In addition, interleaved T2-weighted sections might be of value. New imaging techniques that allow thinner sections while maintaining adequate signal to noise (A. Litt, "Ultra High Resolution T2-Weighted MR Imaging of the Seventh and Eighth Cranial Nerves"; S. Rand, "MR Cisternography of the Cerebellopontine Angle with a High Resolution T2W 3D Fast Spin Echo Technique"; and D. Rubenstein, "Anatomy of the Facial and Vestibulocochlear Nerves in the Internal Auditory Canal"; all presented at the 33rd Annual Meeting of the American Society of Neuroradiology, Chicago, Ill, April 1995) may solve the problems associated with detecting very small lesions on T2-weighted images.

For T2-weighted MR imaging to be an effective screening tool, any subtle abnormality of the nerves, incompletely visible nerves, or questionable hypointensity would undergo contrast-enhanced imaging to avoid delayed diagnosis of small lesions. It would be helpful to use T2-weighted imaging and noncontrast and contrast-enhanced T1-weighted imaging to examine a large patient cohort in the future in a double-blind, prospective study to determine the most sensitive and cost-effective means for screening masses of the IAC. The data from the current study suggest that fast spin-echo T2-weighted imaging with very long TR/TE, when combined with unenhanced T1-weighted imaging, is a potentially useful screening tool for the evaluation of IAC masses, and, as such, merits further study.

References

1. Curati W, Graif M, Kingsley D, Niendorf H, Young I. Acoustic neuromas:Gd-DTPA enhancement in MR imaging. *Radiology* 1986;158:447–451
2. Daniels D, Millen S, Meyer G, et al. MR detection of tumor in the internal auditory canal. *AJNR Am J Neuroradiol* 1987;8:249–252
3. Stack J, Ramsden R, Antoun N, Lye R, Isherwood I, Jenkins J. Magnetic resonance imaging of acoustic neuromas: the role of gadolinium-DTPA. *Br J Radiol* 1988;61:800–805
4. Lhuillier F, Doyon D, Halimi P, Sigal R, Sterkers J. Magnetic resonance imaging of acoustic neuromas: pitfalls and differential diagnosis. *Neuroradiology* 1992;34:144–149
5. Press G, Hesselink J. MR Imaging of cerebellopontine angle and internal auditory canal lesions at 1.5 T. *AJNR Am J Neuroradiol* 1988;9:241–251
6. Enzmann D, O'Donohue J. Optimizing MR imaging for detecting small tumors in the cerebellopontine angle and internal auditory canal. *AJNR Am J Neuroradiol* 1987;8:99–106

7. Valvassori G, Garcia Morales F, Palacios E, Dobben G. MR of the normal and abnormal internal auditory canal. *AJNR Am J Neuroradiol* 1988;9:115–119
8. Armington W, Harnsberger H, Smoker W, Osborn A. Normal and diseased acoustic pathway: evaluation with MR imaging. *Radiology* 1988;167:509–515
9. Renowden S, Anslow P. The effective use of magnetic resonance imaging in the diagnosis of acoustic neuromas. *Clin Radiol* 1993; 48:25–28
10. Phelps P. Fast spin echo MRI in otology. *J Laryngol Otol* 1994; 108:383–394
11. Kasantikul V, Netsky M, Glasscock M, Hays J. Acoustic neurilemmoma: clinicoanatomic study of 103 patients. *J Neurosurg* 1980; 52:28–35
12. Atlas S. Intraaxial brain tumors. In: Atlas S, ed. *Magnetic Resonance Imaging of the Brain and Spine*. New York, NY: Raven Press; 1991:305
13. Som P. Salivary glands. In: Som P Bergeron R, eds. *Head and Neck Imaging*. St Louis, Mo: Mosby-Year Book; 1991:292
14. Mafee M. Acoustic neuroma and other acoustic nerve disorders. *Semin Ultrasound CT MR* 1987;8:256–283
15. Curtin H. CT of acoustic neuroma and other tumors of the ear. *Radiol Clin North Am* 1984;22:77–105
16. Rubinstein L. *Tumors of the Central Nervous System*. Washington, DC: Armed Forces Institute of Pathology; 1972:207
17. DiTullio M, Malkasian D, Rand R. A critical comparison of neurosurgical and otolaryngological approaches to acoustic neuromas. *J Neurosurg* 1978;48:1–12
18. Jackler R. *Acoustic neuroma (vestibular schwannoma)*. In: Jackler R, Brackmann DE, eds. *Neurotology*. St Louis, Mo: Mosby-Year Book; 1994:729–785
19. Goodhill V. Lesions of the eighth nerve, petrous apex, and cerebellopontine angle. In: Goodhill V, ed. *Ear Diseases, Deafness, and Dizziness*. Hagerstown, Md: Harper & Row; 1979:491–502
20. Tallan E, Harner S, Beatty C. Does the distribution of Schwann cells correlate with the observed occurrence of acoustic neuromas? *Am J Otol* 1993;14:131–134
21. Brackmann D, Arriaga M. Differential diagnosis of neoplasms of the posterior fossa. In: Cunnings C, ed. *Otolaryngology–Head and Neck Surgery*. St Louis, Mo: Mosby-Year Book; 1993:3271–3291
22. Schuknecht H. Neoplastic growth. In: Schuknecht H, ed. *Pathology of the Ear*. Cambridge, Mass: Harvard University Press; 1974: 415–451
23. Martuza R, Ojemann R. Bilateral acoustic neuromas: clinical aspects, pathogenesis and treatment. *Neurosurgery* 1982;10:1–12
24. Hardy M, Crowe S. Early asymptomatic acoustic tumor. *Arch Surg* 1936;32:292–301
25. Sterkers J, Perre J, Viala P, Foncin J-P. The origin of acoustic neuromas. *Acta Otolaryngol (Stockh)* 1987;103:427–431
26. Duvoisin B, Fernandes J, Doyon D, Denys A, Sterkers J-M, Bobin S. Magnetic resonance findings in 92 acoustic neuromas. *Eur J Radiol* 1991;13:96–102
27. Jackler R, Shapiro M, Dillon W, Pitts L, Lanser M. Gadolinium-DTPA enhanced magnetic resonance imaging in acoustic neuroma diagnosis and management. *Otolaryngol Head Neck Surg* 1990;102:670–677
28. Cohen T, Powers S, Williams DI. MR appearance of intracanalicular eighth nerve lipoma. *AJNR Am J Neuroradiol* 1992;13:1188–1190

Please see the Commentary on page 1226 in this issue.